Micro-Raman/PL and Micro-LBIC studies of CZTSe materials and PV devices

Conference Paper *in* Conference Record of the IEEE Photovoltaic Specialists Conference · June 2013
DOI: 10.1109/PVSC.2013.6744998

3 authors:

Qiong Chen
University of North Carolina at Charlotte
15 PUBLICATIONS **10** CITATIONS
SEE PROFILE

Naili Yue
MicroVision
20 PUBLICATIONS **96** CITATIONS
SEE PROFILE

Yong Zhang
University of North Carolina at Charlotte
227 PUBLICATIONS **3,946** CITATIONS
SEE PROFILE

Micro-Raman/PL and Micro-LBIC Studies of CZTSe Materials and PV Devices

Qiong Chen, Naili Yue, and Yong Zhang

Electrical and Computer Engineering Department
Energy Production and Infrastructure Center
University of North Carolina at Charlotte, Charlotte, NC

***Abstract*—Micro-Raman/PL/LBIC (Laser Beam Induced Current) was applied to investigate the homogeneity of polycrystalline $Cu_2ZnSnSe_4$ (CZTSe) thin-films from both front surface and cleaved edge with sub-micron spatial resolution. By comparing the materials before and after CdS coating, we have investigated the effect of non-uniformity of CdS layer on the spatial variation of the photo-response, correlating to the μ-Raman/PL probes. The CdS induced spatial variation is found to be a source of inhomogeneity in addition to that of the absorber layer itself. The devices investigated typically have $> 8.5\%$ efficiency. The contrast of the LBIC signal adjacent to the CdS rich area is found to depend on excitation laser power, indicating a potential for further efficiency improvement. Cleaved edge Raman probe has revealed possible variation in the compositions along the growth direction.**

***Index Terms*—CZTSe, CdS, thin film, solar cell, LBIC Micro-Raman, cleaved edge.**

I. Introduction

$Cu_2ZnSn(S,Se)_4$ (CZTSSe) is a quaternary compound which contains earth-abundant and nontoxic elements. It is considered as one of the most promising absorber materials for thin film solar cells. Many methods have been developed to fabricate CZTSSe based thin film solar cells to achieve higher efficiency and/or at lower cost since its debut in 1996 [1]. Recently, $> 11\%$ efficiency has been reported for CZT(S,Se) cells [2], and $> 9\%$ for CZTSe [3].

The presence of the secondary phases and other sources of homogeneity are expected to affect the device performance. Even the inhomogeneity on micron and sub-micron scale is expected to be important for device performance [2]. In this work, we examined the homogeneity of the CZTSe thin film and device, from both front surface and cleaved edge, using micro-Raman, PL as well as micro-LBIC with sub-micron spatial resolution. We investigate the impact of inhomogeneity in both the absorber layer and CdS window layer on the device performance by correlating the three spatially resolved measurements performed in the same area with better than 0.5 μm spatial resolution. Cleaved-edge probe offers non-destructive study of the depth profile of the material composition, and complementary probe of the lateral variation to the traditional front surface measurement.

II. Experimental Details

Micro-Raman/PL spectroscopy was performed with a Horiba Jobin Yvon HR800 confocal Raman system using a 532 nm laser as the excitation source. The laser power was kept less than 0.3 mW in order to avoid any thermal effect or material damage. When a 100x objective lens is used, the laser spot size is ~ 0.72 μm, and the spatial resolution is about half of that. For the LBIC measurement, gold plated probes were used to conduct the photo-current from the devices. The laser is modulated by a mechanical chopper, and the LBIC signal is measured by a SR lock-in amplifier with a SP low noise current pre-amplifier.

Three samples were measured: M12 bare CZTSe film without CdS coating, M22 CZTSe device processed from the same film (M12), and M23 CZTSe device from a different but similar film. All the CZTSe films were grown using a vacuum co-evaporation method, and the devices investigated have larger than 8.5% efficiencies. The film thickness is approximately 1 μm. The details for the film growth and device fabrication can be found in [3]. The measurements were performed at room temperature.

III. Experimental Result

Three distinctly different types of areas on the device M22 and M23 front surface were found under optical microscope: bright spot, dark spot and general area. The typical sizes of the bright and dark spots are around 1-2 μm. However, no bright spot was found on the bare sample M12. Fig. 1 shows typical Raman spectra from the three types of spots. In addition to 172 cm^{-1} and 196 cm^{-1} CZTSe related Raman peaks [4], both CZTSe devices M22 and M23 give rise to a 303 cm^{-1} Raman peak in all the three spots, but this peak was observed neither in the dark spot nor the general area Raman spectra of sample M12 which was not coated with CdS. The CZTSe Raman peaks from all the spots of three samples have similar peak shape and intensity. Since the 303 cm^{-1} only appears in the finished devices, it is neither CZTSe related nor from any secondary phase in the CZTSe film. By noticing that the excitation laser energy is rather close to the bandgap of CdS and Raman shift is also very closely matched that CdS LO phonon, the 303 cm^{-1} peak can be attributed to the LO phonon mode of CdS [5], which is further supported by the appearance of another weaker peak near 600 cm^{-1} that also matched the seond order LO phonon Raman of CdS [5]. The intensity of the 303 cm^{-1} is the weakest for the general spot relative to the CZTSe peak, comparable to that of the CZTSe peak for the dark spot, but becomes more than five times as

978-1-4799-3299-3/13/$31.00 ©2013 IEEE

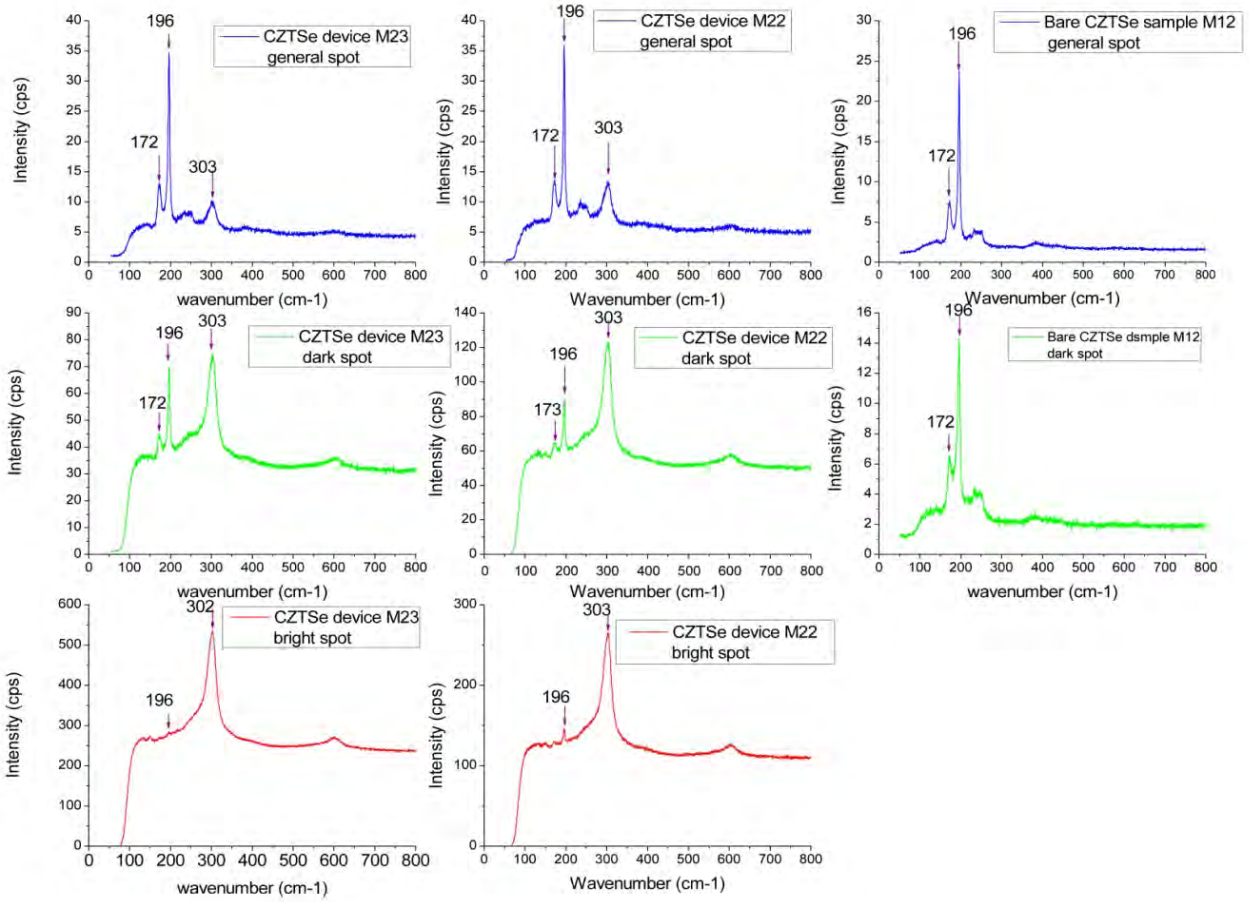

Fig. 1. Raman spectra from general spot, dark spot and bright spot of sample M23, M22 and M12.

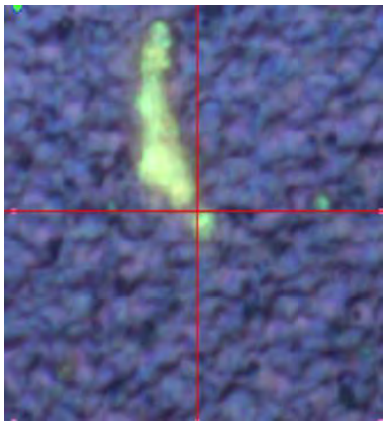

Fig. 2. Optical image of M23 surface mapping area.

strong for the bright spot in M22, and ten times in M23. These observations suggest that both the dark and bright spots are CdS rich compared to the general area, even richer for the bright spot. The comparison between M22 and M23 seems to suggest that the CdS layer at the bright spot could be somewhat thicker in M23 than in M22. Fig. 2 is an optical image for an area containing a bright spot in device M23. Fig. 3 shows the intensity map of a 20 μm x 20 μm area, the same as shown in Fig. 2, for the 303 cm^{-1} Raman peak. The measurement step size is 0.25 μm. The red area with stronger Raman intensity in Fig. 3 has a similar shape with that of the bright area in the optical image, which indicates that the bright spot is CdS rich. Therefore, the 303 cm^{-1} Raman peak intensity variation on the device front surface can be related to the spatial variation of CdS layer thickness.

In general, LBIC mapping reflects the overall inhomogeneity of the device including the contribution from both the absorber and supporting layers. We have found that the photo-current at the CdS-rich bright spot yield either higher or lower photo-current than the average area, respectively, with high or low excitation laser power. Fig. 4 to Fig.7 show the LBIC mapping data and the histograms of the data from the same area used in Fig. 3 with about 2 μW and 200 μW incident laser power. The change (reversal) in the contrast between the CdS rich and the general regions is apparent when we compare

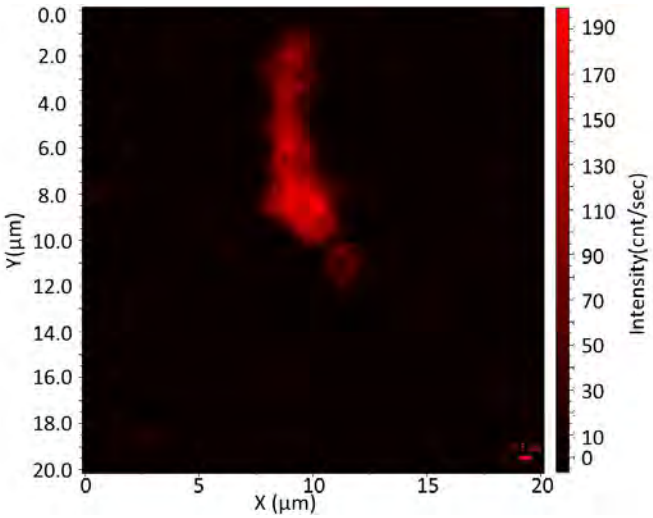

Fig. 3. M23 surface Raman mapping.

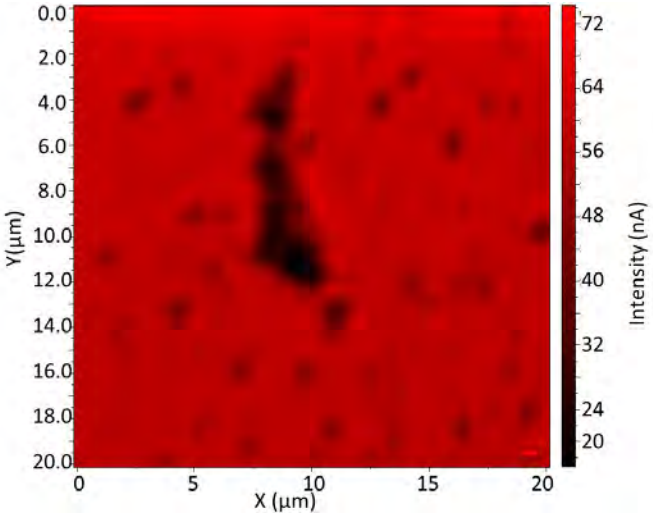

Fig. 4. M23 surface LBIC mapping with 2 μW 532 nm laser.

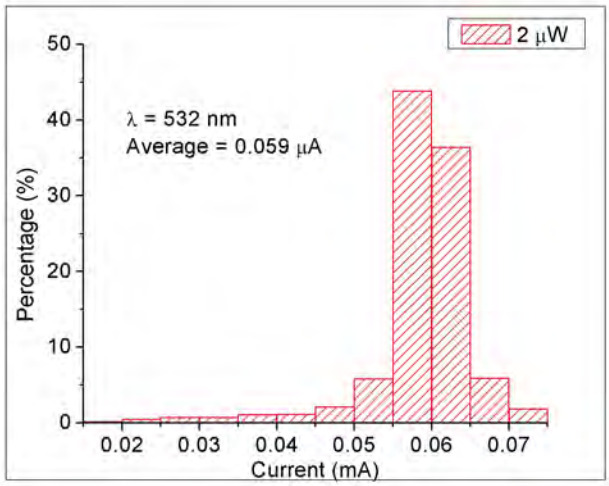

Fig. 5. Histogram of 2 μW LBIC mapping.

Fig. 4 and Fig. 6. The shape of the abnormal region appears to have a similar shape with that in the optical image as well as the Raman map. Fig. 5 and Fig. 7 show respectively the histogram plots under 2 and 200 μW. We notice that while the laser power increases by 100 times from Fig. 4 to Fig. 6, the average current has increased by a little more than 10 times, whereas the current from the CdS rich region has increased by a factor close to that of the laser power, which leads to the reversal of the contrast. This finding suggests that the quantum efficiency of the average area has degraded significantly under high illumination power, but the area with thicker CdS layer shows very little or no degradation in quantum efficiency.

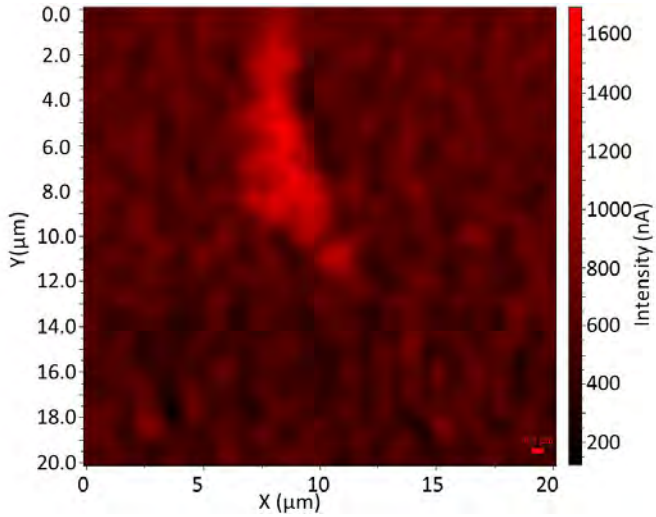

Fig. 6. M23 surface LBIC mapping with 200 μW 532 nm laser.

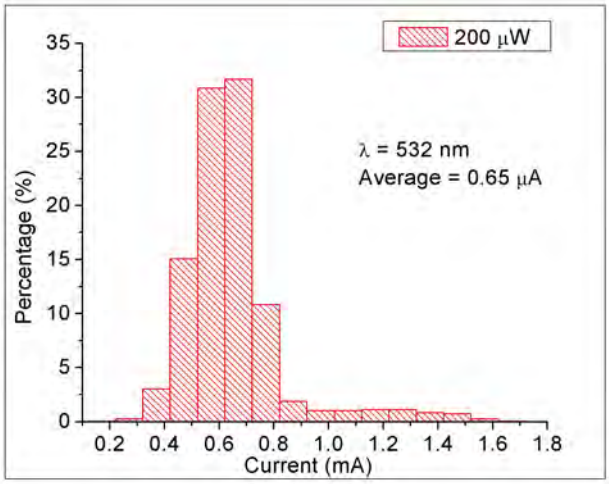

Fig. 7. Histogram of 200 μW LBIC mapping.

We have also measured the local I-V curves at different spots with 200 μW excitation (shown in Fig. 8), and notice that spots with larger photo-currents usually also yield larger open circuit voltages, thus leading to higher local energy

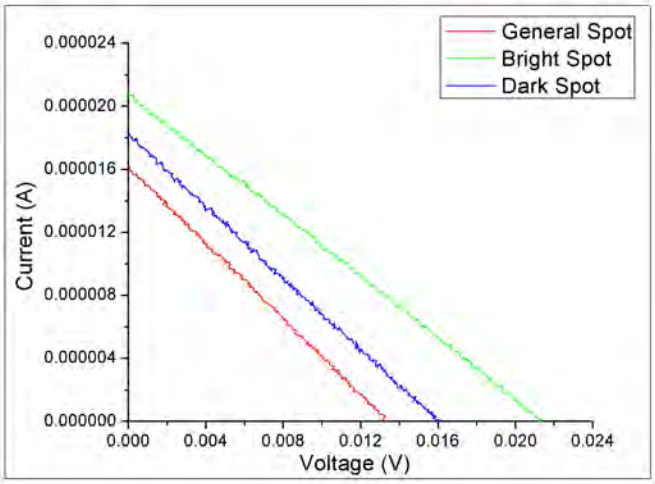

Fig. 8. M23 three types of spots local I-V measurement.

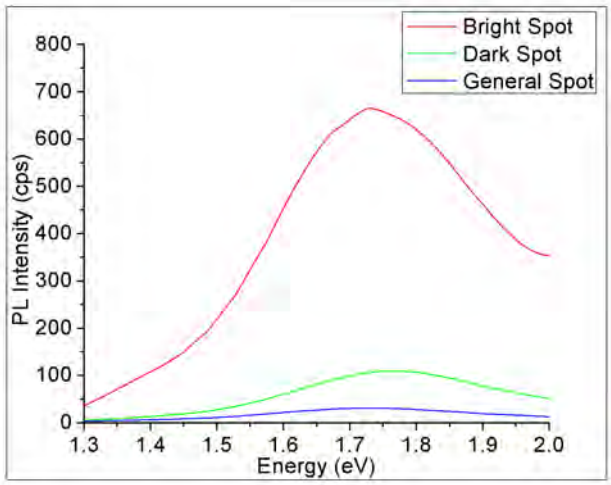

Fig. 10. M23 PL spectra from three different types of spots.

conversion efficiencies. In other words, the non-uniformity of the LBIC distribution indicates the potential for further efficiencicy improvement, if the material could be optimized to be the same as those "star" areas, although it does not necessarily mean that the same scale of improvement for the macroscopic device performance. In this case, a thicker CdS layer might improve the device performance under high illumination level, for instance, under concentration.

Cleaved edge Raman study was also performed on device M22 with results shown in Fig. 9. One can clearly see the variation of the spectral features with the film depth. In addition to the 196 cm^{-1} and 170 cm^{-1} peaks close to those observed CZTSe features from the front surface, we have observed a number of more Raman peaks whose origins are yet to be determined.

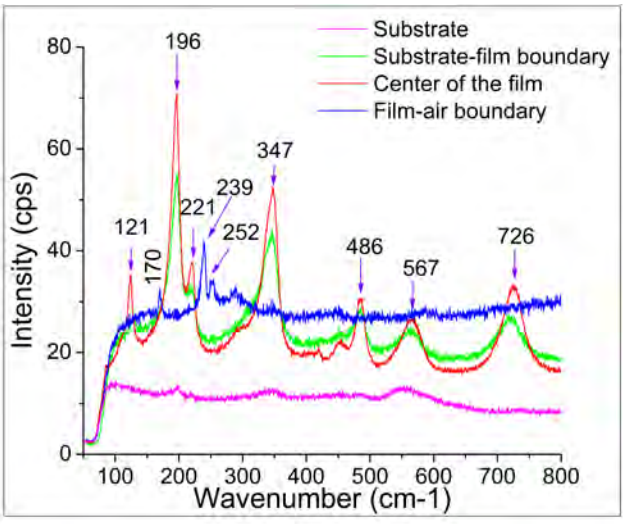

Fig. 9. Raman spectra of the film measured from the cleaved edge.

PL spectra from three typical areas for device M23 are

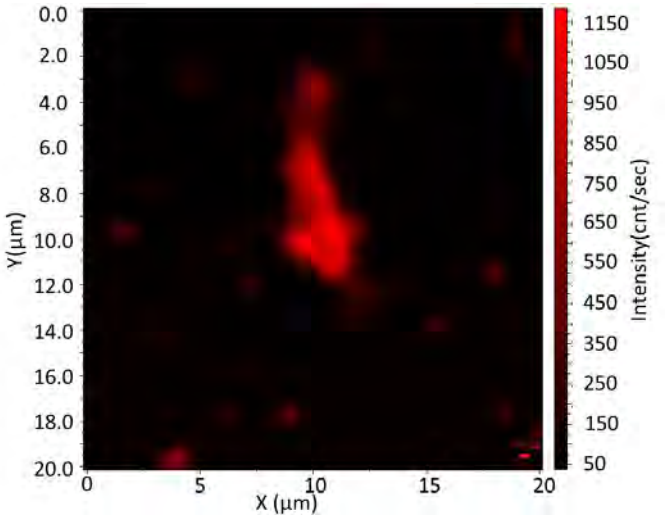

Fig. 11. M23 surface PL mapping.

compared in Fig. 10. They are measured for the spectra range above the bandgap of CZTSe which is around 1.0 eV [4], because fo the limitation of the CCD spectral response in our system. A broad PL band is observed far above the bandgap of CZTSe with peak energy varying slightly from 1.73 eV for the general spot, 1.77 eV for the dark spot, and 1.73 eV for the bright spot. A PL map in Fig. 11 also shows strong PL intensity within the bright CdS rich area, which confirms the inhomogeneity of the CdS layer.

IV. Discussion

CZTSe films before and after CdS coating were examined by Micro-Raman/PL/LBIC, which revealed the spatial variation of the material composition and the impact on the local photo-response in both short-circuit current (I_{sc}) and open-circuit voltage (V_{oc}). CZTSe signature Raman peaks 172 cm^{-1} and 196 cm^{-1} were observed. By comparing Raman

spectra, we have found that CZTSe devices contain areas with surplus CdS. With Raman spectroscopy, we have identified three distinct types of areas on the device front surface: CdS-rich bright area with strong 303 cm^{-1} CdS LO phonon peak, general CZTSe area with weak 303 cm^{-1} peak, and dark spot that is also CdS rich but less than the bright area. The PL spectra provide complementary information of the film chemical compositions. The statistical distribution of the LBIC mapping shows the microscopic scale photo-current variation that can be due to the material inhomogeneity in either the absorber layer or CdS layer. The local I-V measurement has shown that a high I_{sc} spot typically shows high V_{oc}. Future effort would be to identify the chemical compositions and structural parameters of the "star" regions, and attempt to produce the same uniform material; and to correlate the device performance under local excitation and uniform illumination in order to better predict the implication of the spatial variation of the local excitation on the device performance under actual operating condition. Cleaved edge μ-Raman/PL/LBIC measurements offer an alternative and nondestructive evaluation of the device uniformity and potentially may be able to probe the domain boundary when the domain sizes become somewhat bigger than the typical sizes of the current materials.

ACKNOWLEDGMENT

We greatly appreciate Dr. I. Repins (NREL) for kindly providing the samples and valuable comments, and thank Dr. S. Choi (NREL) for very helpful discussions on Raman data. YZ acknowledges the support of Bissell Distinguished Professorship.

REFERENCES

[1] H.Katagiri, N.Sasaguchi, S.Hando, S.Hoshino, J.Ohashi, and T. Yokota, "Preparation and evaluation of Cu_2ZnSnS_4 thin films by sulfurization of E-B evaporated precursors",*in the 9th International Photovaltaic Science and Engineering Conference*, p.745, 1996.

[2] T.K.Todorov, J.Tang, S.Bag, O.Gunawan, T.Gokmen, Y.Zhu, and D.B.Mitzi, "Beyond 11% efficiency: characteristics of state-of-the-art $Cu_2ZnSn(S,Se)_4$ solar cells", *Advanced Energy Materials*,vol. 3, pp. 34-38, 2013.

[3] I.Repins, C.Beall, N.Vora, C.Dehart, D.Kuciauskas, P.Dippo, B.To, J.Mann, W.Hsu, A.Goodrich, and R. Noufi,"Co-evaporated $Cu_2ZnSn(S,Se)_4$ films and devices" *Solar Energy Materials & Solar cells*,vol. 101, pp. 154-159, 2012.

[4] M.Grossberg, J.Krustok, J.Raudoja, K.Timmo, M.Altosaar and T.Raadik, "Photoluminescence and Raman study of $Cu_2ZnSn(Se_xS_{1-x})_4$ monograins for photovoltaic applications", *Thin Solid Films*, vol. 519, pp. 7403-7406, 2001.

[5] R.C.C.Leite, J.F.Scott, and T.C.Damen, "Multiple-Phonon resonant Raman scattering in CdS", *Phys. Rev. Lett.*, vol. 22, pp. 780-782, 1969